University of Baghdad
College of Engineering
JE
JOURNAL OF ENGINEERING

Journal of Engineering
journal homepage: www.joe.uobaghdad.edu.iq
Number 12 Volume 25 December 2019

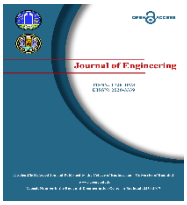

Electrical, Electronics and communications, and Computer Engineering

A Neural Networks based Predictive Voltage-Tracking Controller Design for Proton Exchange Membrane Fuel Cell Model

Ahmed S. Al-Araji
Computer Engineering Department
University of Technology
Baghdad, Iraq
Email:60166@uotechnology.edu.iq

Hayder A. Dhahad
Mechanical Engineering Department
University of Technology
Baghdad-Iraq
E-mail:hayder_abed2002@yahoo.com

Essra A. Jaber
Control and Systems Engineering Department
University of Technology
Baghdad-Iraq
E-mail:esraabbas599@gmail.com

ABSTRACT

In this work, a new development of predictive voltage-tracking control algorithm for Proton Exchange Membrane Fuel Cell (PEMFCs) model, using a neural network technique based on-line auto-tuning intelligent algorithm was proposed. The aim of proposed robust feedback nonlinear neural predictive voltage controller is to find precisely and quickly the optimal hydrogen partial pressure action to control the stack terminal voltage of the (PEMFC) model for N-step ahead prediction. The Chaotic Particle Swarm Optimization (CPSO) implemented as a stable and robust on-line auto-tune algorithm to find the optimal weights for the proposed predictive neural network controller to improve system performance in terms of fast-tracking desired voltage and less energy consumption through investigating and comparing under random current variations with the minimum number of fitness evaluation less than 20 iterations.

Keywords: Neural Networks, Predictive Controller, Fuel Cell, Particle Swarm Optimization.

الشبكات العصبية اساس تصميم مسيطر تتابع الجهد التنبؤي لنموذج خلية الوقود غشاء تبادل البروتون

احمد صباح الاعرجي
استاذ دكتور
قسم هندسة الحاسوب-الجامعة التكنولوجية

حيدر عبد ضهد
استاذ مساعد دكتور
قسم هندسة الميكانيك-الجامعة التكنولوجية

اسراء عباس جبر
ماجستير
قسم هندسة السيطرة والنظم-الجامعة التكنولوجية

الخلاصة

في هذا العمل, تم اقتراح تطوير خوارزمية جديدة للتحكم في تتبع الجهد التنبؤي لنموذج خلية وقود غشاء تبادل البروتون (PEMFCs) بأستخدام تقنية الشبكة العصبية المستندة على الخوارزمية الذكية ذات التنغيم التلقائي وبشكل حي ومتصل. ان الهدف من المسيطر الجهد التنبؤي العصبي اللاخطي المتين ذات التغذية العكسية المقترح هو ايجاد امثلية فعل الضغط الجزئي للهيدروجين للسيطرة على فولطية الخرج لنموذج (PEMFC) لعددة خطوات تنبؤية على وجه التحديد وبسرعة. لقد تم تنفيذ حشد الجيسيمات الامثلية الفوضوية (CPSO) كخوارزمية مستقره ومتينة ذات التنغيم التلقائي وبشكل حي متصل

*Corresponding author
Peer review under the responsibility of University of Baghdad.
https://doi.org/10.31026/j.eng.2019.12.03

Article received: 23/1/2019
Article accepted: 9/2/2019
Article published: 1/12/2019

للحصول على الاوزان المثلى للمسيطر الشبكة العصبية التنبؤية المقترح لتحسين اداء النظام من حيث سرعة تتابع الفولطية المطلوبة وتقليل خسائر الطاقة من خلال التحقيق والمقارنة تحت تغيرات العشوائية للتيار مع اقل عدد لدالة التقييم اقل من 20 تكرار.

الكلمات الرئيسية: الشبكات العصبية, المسيطر التنبؤي, خلية الوقود, امثلية حشد الجسيمات.

1. INTRODUCTION

In recent years, fuel cells are considered as one of the modern technologies for alternative power generation in the future, because of their clean power source with zero-emission, quiet operation, high efficiency and system robustness **Ziogou, et al., 2018**.

In general, fuel cells have static energy, and they are electrochemical cells that can generate electrical energy from chemical reaction by continuously processing the cell with hydrogen and oxygen, this is distinguished from other sources of electricity generation such as batteries and internal combustion engine **Daud, et al., 2017**. A fuel cell consists of two components: two electrodes (anode and cathode respectively) and electrolyte sandwiched between electrodes. The electrodes material is porous covered with catalyst. A single fuel cell produces one volt for the voltage required must connect more than one cell in either parallel or series. The fuel cells are classified according to the kind of electrolyte to direct methanol fuel cell; alkaline fuel cell; phosphoric acid fuel cells; molten carbonate fuel cell; solid oxide fuel cell; reversible fuel cell and proton exchange membrane fuel cells (PEMFCs) **El-Sharkh, et al., 2004**. The PEMFC systems have drawn a lot of interest for the researchers recently because they have many qualifications such as these cells can operate at lower temperatures, lower pressures, quick start-up, quiet operation, small size and high efficiency that recognized from other fuel cells **Rajasekar, et al., 2015**. To keep the PEMFC systems operating at the maximum power point conversion, researchers have proposed many control methods for tracking the output voltage of the fuel cell stack when the load current variable such as: adaptive fuzzy logic controller **Benchouia, et al., 2015**, optimal PID with fuzzy controller **Beirami, et al., 2015**, second-order sliding mode controller **Liua, et al., 2015**, adaptive back-stepping controller **Li, et al., 2011**, neural networks controller **Abbaspour, et al., 2016**, PID neural controller **Damour, et al., 2014**, nonlinear model predictive controller **Ziogoua, et al., 2013** and others. As well as many types of intelligent evolutionary algorithms are used to represent the modelling of the PEMFC system in the simulation in order to understand the involved phenomena of the fuel cell such as: PSO algorithm **Salim, et al., 2013**, modified PSO algorithm **Isa and Rahim, 2013**, honey bee mating optimization algorithm **Manikandan and Ramalingam, 2016** artificial bee swarm optimization algorithm **Askarzazeh and Rezazadeh, 2011**, firefly optimization algorithm **Ali, et al., 2018**, genetic optimization algorithm **Kumar, et al., 2017**. The motivation of this paper is to focus on the dynamic response of the PEM fuel cell stack and stabilize the power output, especially when it is used in mobile applications. Furthermore, the modeling representation of the PEMFC system and controlling the output voltage are still challenging issue. The main contribution of this paper is to:

- Study and analyze the PEM fuel cell operating system in terms of the effect of each variable input-output such as hydrogen partial pressure, temperature and load current.
- Build the neural networks identifier PEMFC model based on the five steps identification technique with off-line and on-line CPSO algorithm for overcoming the modeling challenge and obtaining fast learning; no oscillation in the output identifier model and minimum number of fitness evaluation.
- Derive a numerical feedforward controller to keep the steady-state tracking voltage error of the fuel cell stack to zero value.
- Design of a neural feedback controller with prediction algorithm for N-step ahead to stabilize and track desired output voltage of the fuel cell system in the transient state as well as to get the optimal value of the hydrogen partial pressure control effort.
- Improve and stabilize the output voltage performance of the PEMFC system and the hydrogen partial pressure control effort because it uses multi-objective cost function.

2. NONLINEAR MODEL OF PROTON EXCHANGE MEMBRANE FUEL CELLS

In general, PEM fuel cells use a solid polymer as an electrolyte and porous carbon electrodes containing a platinum or platinum alloy catalyst as shown in **Fig. 1.** The electrode is made up of platinum also, so this kind is of high cost **Derbeli, et al., 2017**. PEMFCs are used for transportation and stationary application since this kind of cells consider most promising power generator and can offer clean power source **Derbeli, et al., 2017**.

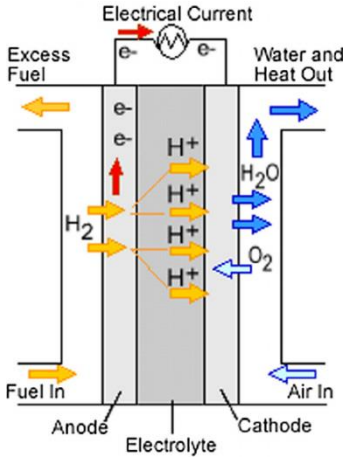

Figure 1. The principle working of PEMFCs, **Derbeli, et al. 2017**.

The hydrogen gas enters the system from anode side, due to the presence of platinum catalyst, hydrogen gas decomposes into electrons and protons. Only protons transport through membrane to the other side (cathode) **Benchouia, et al., 2015, Beirami, et al., 2015, and Derbeli, et al., 2017**.

The chemical reaction at anode is:

$$2H_2 \rightarrow 4H^+ + 4e^- \quad (1)$$

Electrons pass through the external electrical circuit to generate electric signal. In cathode side, the electrons and protons react with oxygen from air to produce water and heat as result of reaction **Benchouia, et al., 2015, Beirami, et al., 2015, and Derbeli, et al., 2017**.

The chemical reaction at cathode is:

$$4e^- + 4H^+ + O_2 \rightarrow 2H_2O \quad (2)$$

Water produced must be thrown out to keep system from flooding and rendering inoperative passive. Output power produced from single-cell is (1 volt), so to get the desired power must connect cells in either parallel or series to convert names to stack fuel cell. The temperature work of this kind of fuel cells around (50-100 C^o) **Benchouia, et al., 2015, Beirami, et al., 2015, and Derbeli, et al., 2017**.

The performance of fuel cell can be obtained by using a polarization curve that explains the nonlinear characteristics between voltage and load current (V-I). To calculate the steady-state V-I of fuel cell used **Benchouia, et al., 2015, Beirami, et al., 2015, and Derbeli, et al., 2017**.

$$V_{cell} = V_{steady} - V_{transient} \quad (3)$$

$$V_{steady} = E_N - V_{ohm} \quad (4)$$

$$V_{transient} = V_{act} + V_{con} \quad (5)$$

Where: Vcell: represents the output voltage of the fuel cell. EN: represents thermodynamic potential. Vact: is the voltage drop due to the activation of the anode and cathode. Vcon: is the concentration overvoltage. Vohm: represents voltage descent resulting from the impedance of the conduction of protons through the electrolyte and of the electrons through its track.

Physical parameters and the characteristic of the PEMFC are taken from **Correa, et al., 2003** as shown in **Table 1**.

Table 1. The physical and characteristics of fuel cell **Correa, et al., 2003**.

Parameters	Values	Units
N_{cell}	32	--
T	298	Kelvin degree
A	64	cm^2
L	$178 * 10^{-6}$	cm
PH_2	1-5	Atm
PO_2	0.2	Atm
R_c	0.0003	**Ω**
β	0.0169	V
α_1	0.948	--
α_2	-0.00312	--
α_3	$-7.6 * 10^{-5}$	--
α_4	$1.93 * 10^{-4}$	
J	0.0073	mA/cm^2
J_{max}	0.469	mA/cm^2
Φ	23	--

The thermodynamic potential (E_N) represents the ideal output voltage, thus to determine it, Eq. (6) is used, **Correa, et al., 2003**:

$$E_N = 1.229 - 0.85 * 10^{-3} * (T - 298) + 4.3085 * 10^{-5} * T * ((lnPH_2) + 0.5 * \ln(PO_2)) \quad (6)$$

Where:PH_2: is the hydrogen partial pressure. PO_2: is the oxygen partial pressure.
Activation loss is the voltage drop due to the energized between the anode and cathode, **Correa, et al., 2003**.

To determine this type of loss, Eq. (7) can be used:

$$V_{act} = \alpha_1 + \alpha_2 * T + \alpha_3 * T * \ln(CO_2) + \alpha_4 * T * \ln(I) \quad (7)$$

where I: is the load current. CO_2: is the dissolved oxygen concentration in the surface of cathode om /cm^3.
By using Henry law CO_2 as Eq. (8)**, Correa, et al., 2003.**

$$CO\_2 = (PO\_2)/(5.08 * \ 〚10〛\ ^6 * \exp((-498)/T)) \quad (8)$$

To determine the ohmic loss voltage, Eq. (9) is used, **Derbeli, et al., 2017 and Correa, et al., 2003.**

$$V_{ohm} = I * (R_c + R_m) \quad (9)$$

Where, R_m: is the equivalent resistance of electron flow. R_c: is the constant value of proton resistance.

$$R\_m = (\rho\_(m\ ) L)/A \quad (10)$$

where ρ_m: is the represent the specific resistance of membrane and can be determined by using Eq. (11):

$$\rho_m = (181.6[1 + 0.03(I/A) + 0.062(T/303)\text{^}(2\quad) * (I/A)\text{^}2.5)/(\Phi - 0.634 - 3(I/A)\ \ 〚exp〛 \text{^}[4.18(T - 303)/T]\ ) \quad (11)$$

Concentration loss calculated by using Eq. (12**), Derbeli, et al., 2017 and Correa, et al., 2003.**

$$V\_con = -\beta \ln\ 〚(1 - J/Jmax〛\ ) \quad (12)$$

where β: is the cell type dependence parameter. J: is the density of current that passes through the cell. Jmax: is the maximum current density pass through the cell, where

$J\_max = Imax/A$ (13)

The overall output voltage of stack can have determined by Eq. (14) **Derbeli, et al., 2017 and Correa, et al., 2003.**

$V\_FC = N\_cell\ V\_cell$ (14)

where Ncell: represents the number of the stack.

The total power of the stack calculated by this Eq. (15):

$Power_{FC} = I\ V_{FC}$ (15)

3. PREDICTIVE NEURAL CONTROLLER DESIGN

Fig. 2 explains the general form of the predictive neural controller for the PEMFC. The proposed predictive neural controller contains three sections: the first section is the on-line neural network identifier. The second section is the numerical feedforward controller. The third section is the feedback controller with optimizer algorithm. In the next sections, each section of the proposed controller will be illustrated in detail.

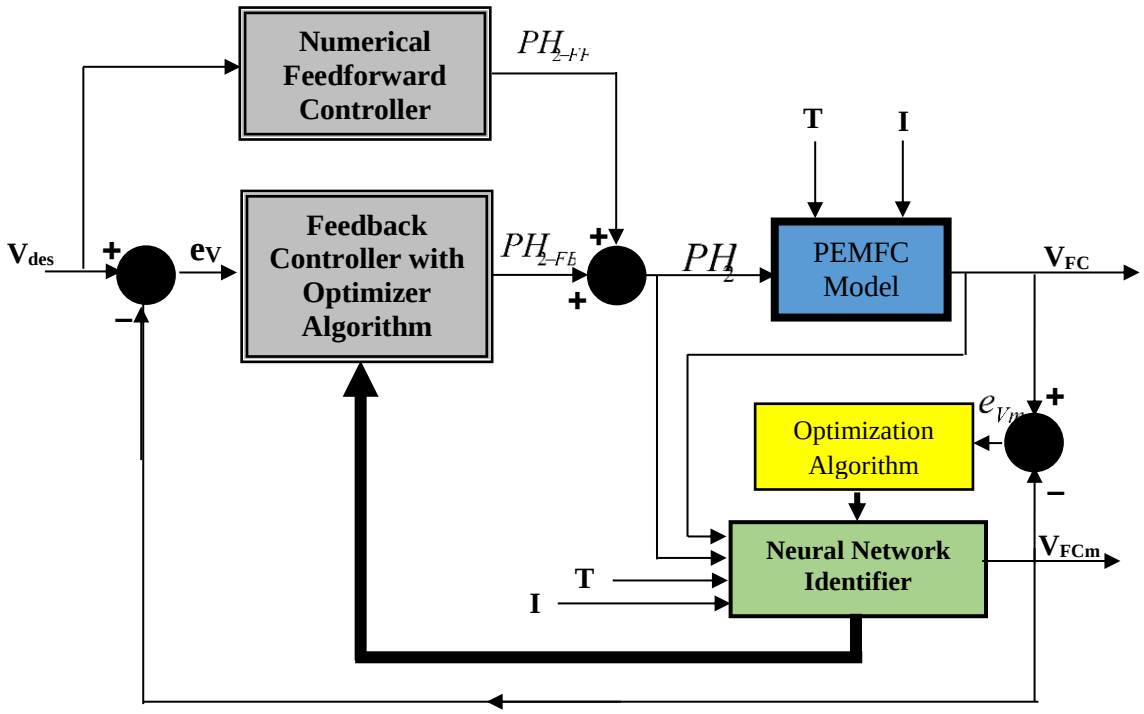

Figure 2. The general structure of the proposed predictive neural controller.

3.1 The On-Line Neural Networks Identifier

The modeling and system identification is the main task of the structure for the proposed controller because it is a require-ding for analysis and controller designing, **Al-Araji, et al., 2011**. The structure of neural identifier algorithm consists of five stages as shown in **Fig. 3 Al-Araji, et al., 2011**. Based on the description of the PEMFC system operational there are three outputs of PEMFC system, the first is the Fuel-Cell stack output voltage (V_{FC}); the second is the temperature (T) variable of the Fuel Cell system operational and the third is the load current (I_L) variation. As well as, there are two inputs of the PEMFC system which controlled the operation of the Fuel Cell, the first one is the hydrogen partial pressure (PH_2) controlled effort and the second is the oxygen partial pressure (PO_2) a constant value in this paper. To represent neural PEMFC model, the Nonlinear Auto Regressive Moving Average (NARMA) **Dagher, 2018** neural network with a Multi-Layer Perceptron (MLP) configuration is used to build the neural network identifier model of the PEMFC system. So the formulated NARMA model of the PEMFC system can be represented as follows:

$$V_{FC}(k+1) = F[V_{FC}(k), \dots, V_{FC}(k-n+1), T(k), \dots, T(k-n+1), I(k), \dots, I(k-n+1), PH_2(k), \dots PH_2(k-n+1)] \quad (16)$$

where F[-]:denotes to the relationship function between the past values of input-output of the fuel cell system.

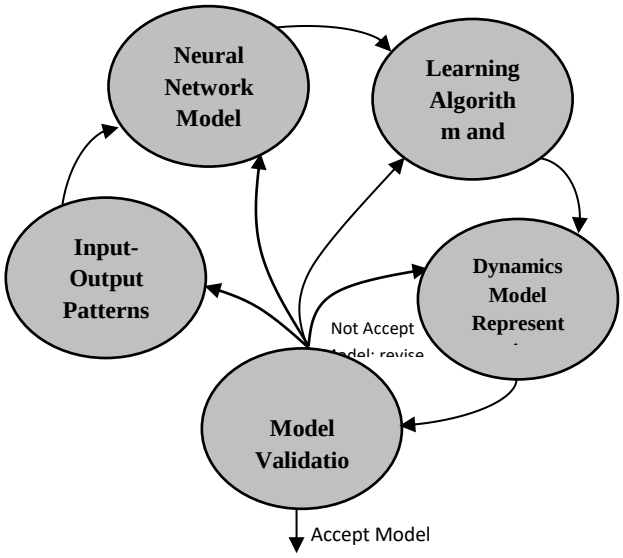

Figure 3. The structure of neural identifier algorithm.

As explained in **Fig. 4,** the proposed dynamic model of MLP neural network (NN) identifier of the PEMFC system is represented in Eq. (17).

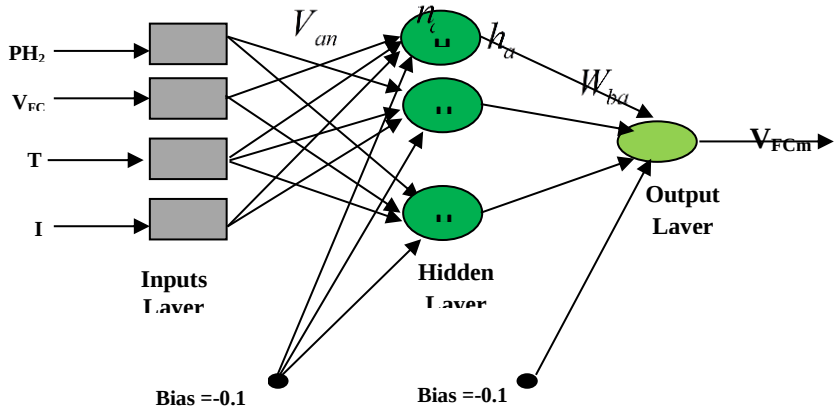

Figure 4. The structure of multi-layered feedforward neural networks

$$V_{FCm}(k+1) = F_m[V_{FC}(k), V_{FC}(k-1), V_{FC}(k-2), T(k), T(k-1), I(k), I(k-1), PH_2(k), PH_2(k-1)] \quad (17)$$

here V_{FCm}: is the neural Fuel-Cell stack output voltage. F_m[-]: denotes the nonlinear relationship function between the past values of input-output of the neural fuel cell system.

The nonlinear relationship of the NN identifier model F_m [-] is the (MLP) model, which means multi-layer perceptron as shown in **Fig. 4,** where it consists of three layers: The input or buffer layer; the hidden or nonlinear activation layer and the output layer. So neural network identifier

weights of the F_m [-] are described as follows: V_{an}: is the weight matrix of the F_m [-] hidden layer. W_{ba}: is the weight matrix of the F_m [-] output layer.
To explain these calculations, consider the general ath neuron in the hidden layer. The inputs to this neuron consist of an nth dimensional vector X , where nth is the number of the input nodes and a bias whose value proposed equal to -0.1, **Al-Araji, et al., 2011** and **Nells, 2001**.
All the inputs have a weight V_{an} linked with it. The first determination within the neuron consists of calculating the weighted sum net_a of the inputs as, **Al-Araji, 2015** and **Nells, 2001**.

$$net_a = [\sum_{a=1}^{Ah} V_{a,n} \times X_n] + V_{a,Ah+1} \times bias \quad (18)$$

Next, the output of the neuron h_a is determined as the continuous sigmoid function of the net_a as:

$$h_a = H(net_a) \quad (19)$$

$$H(net_a) = \frac{2}{1+e^{-net_a}} - 1 \quad (20)$$

After the outputs of the hidden layer are calculated, they are passed into the output layer. In the output layer, a single linear neuron is used to calculate the weighted sum ($neto_b$) of its inputs (the output of the hidden layer as in Eq. (21)), **Al-Araji, et al., 2011** and **Nells, 2001**.

$$neto_b = [\sum_{a=1}^{Ah} W_{b,a} \times h_a] + W_{b,Ah+1} \times bias \quad (21)$$

Where: Ah: called nodes, which mean the number of the hidden neuro, and W_{ba} is the weight between the hidden neuron h_a and the output neuron.
The single linear neuron then passes the sum ($neto_b$) through a linear function of slope 1 or another slope used to scale the output as Eq. (22):

$$V_{FCm} = L(neto_b) \quad (22)$$

here L(x) =x is a linear function of slope 1. (23)
The learning algorithm is usually based on the minimization (with respect to the network weights) of the following objective cost function as in Eq. (24), **Al-Araji, et al., 2011** and **Nells, 2001.**

$$E = \frac{1}{P}\sum_{i=1}^{p}(e^i_{Vm}(k+1))^2 = \frac{1}{P}\sum_{i=1}^{p}(V_{FC}{}^i(k+1) - V_{FCm}{}^i(k+1))^2 \quad (24)$$

where P: represented the number of training points in the training set. $e_{Vm}(k+1)$: denotes prediction model error at each iteration among the true voltage output of the PEMFC and the neural model voltage output. V^i_{FC}: The actual output voltage of the fuel cell of each iteration. V^i_m: represent model output voltage of the neural network of every iteration.
Fig. 5 shows the architecture of a series-parallel identification model based on feedforward MLP neural networks, which is so simple that at each instant of time, the past inputs and the past outputs of the Fuel-Cell system are fed into the neural networks then the network's output yields the prediction error as in Eq. (25). In the model, the inputs of the neural networks model are the output of the actual PEMFC, so this scheme can be used only in conjunction with the system. In this paper, the Particle Swarm Optimization (PSO) as one of the modern stochastic search and an intelligent algorithm is used to learn the identifier neural PEMFC model. PSO is famous by its simple concept, easy implementation, and quick convergence **Salim, et al., 2013, Isa and Rahim, 2013 and Al-Araji, 2015** and the goal of it is to find and tune the best weights neural network to show the effectiveness in terms of number of iterations for evaluating the objective cost function and the minimum value obtained for the mean square error cost function as in Eq. (24). The first step in the PSO algorithm randomly generated particles as initial particles (population of individuals). Each particle is led by the internal interaction in order to get the optimal or near-optimal solution by minimizing the objective cost function by flying through the search space.

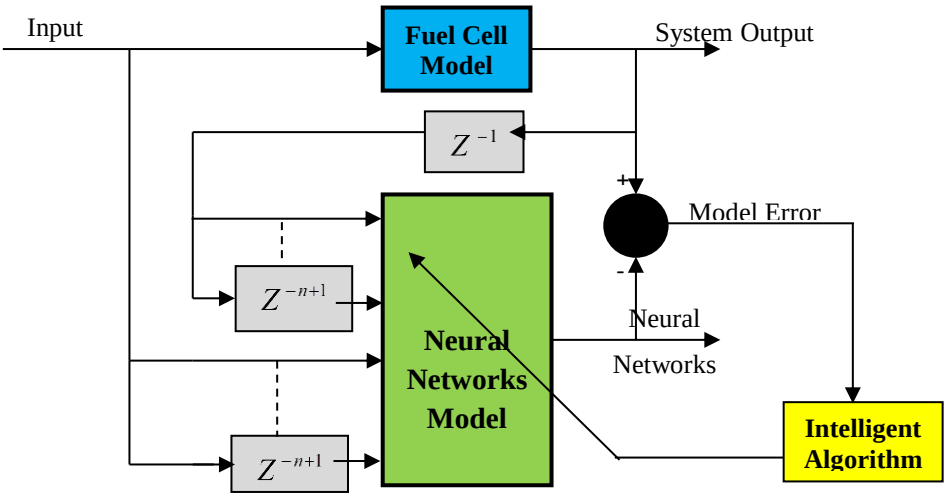

Figure 5. The series-parallel structure model.

In general, to show the movement of particle i, xi, depends on its velocity, Vi, which is adjusted at each time step by using the Global best position, G_{best}, and the Local best position, L_{best}, which have been already found. The particle's velocity update represents as Eq. (25) while the Eq. (26) represents the particle's position update **Salim, et al., 2013, Isa and Rahim, 2013**, and **Al-Araji, 2014**.

$$v_i(k+1) = w.v_i(k) + c_1 r_1[L_{best-i} - x_i(k)] + c_2 r_2[G_{best} - x_i(k)] \quad (25)$$

$$x_i(k+1) = x_i(k) + v_i(k+1) \quad (26)$$

where c_1 and c_2: are cognitive coefficients. r_1 and r_2: are two uniform random numbers.

To modify the operation of PSO algorithm in terms of a random operator in searching and to avoid and solve the global optimization problems with a large number of local minima. The chaotic technique descent because it has been exploited in some metaheuristic methods, which makes it generally exhibits better numerical performance, **Dagher, 2018**.

Therefore, the proposed algorithm is Chaotic Particle Swarm Optimization CPSO algorithm because it has the ability to improve the global searches and reach to an optimal solution with minimum number of iterations that depend on probabilities of the chaotic techniques, **Dagher, 2018** than stochastic techniques. To enhance the capability of PSO in the global searching, it has to put the new inertia weighting in the velocity update equation, and it becomes as follows:

$$v_i(k+1) = w_{new}.v_i(k) + c_1 r_1[L_{best-i} - x_i(k)] + c_2 r_2[G_{best} - x_i(k)] \quad (27)$$

The new inertia weighting in the velocity update Eq. (27) can be calculated by using two steps as follows:

The first step is described the logistic equation employed for constructing chaotic PSO as in Eq. (28) **Dagher, 2018**.

$$\beta(k+1) = \mu\beta(k)[1 - \beta(k)] \quad (28)$$

where μ: is equal to 4 as the control parameter therefore, (0) $\notin$ {0, 0.25, 0.5, 0.75, 1}.

The second step is to find the new weight parameterw_{new}, by using Eqs. (29 and 30) as follows:

$$w = w_{max} - [(w_{max} - w_{min}) \times \frac{iteration(k)}{max.no.iteration}] \quad (29)$$

$$w_{new} = \beta(k+1)w \quad (30)$$

After applying the training mechanism of the neural network, as shown in **Fig. 5** by using CPSO intelligent algorithm for reducing the model error between the actual output voltage $V_{FC}(k+1)$ and neural network model output voltage $V_{FCm}(k+1)$ and is equal to zero approximately then the neural network identifier model will complete the same actual output response.

3.2 The Numerical Feedforward Controller Design

The numerical feedforward controller (NFFC) is very important in the build of proposed predictive neural controller, because of its requisite to keep the steady-state sequence voltage error to zero value, which means that the working of the (NFFC) $PH_{2-FF}(k)$ is to put the output voltage of the PEMFC as the desired input voltage in steady state. Hence, NFFC is assumed to calculate the inverse dynamic of PEMFC system, and so it is called inverse feedforward controller (IFC). To achieve the controller, there are several equations must be numerically calculated as follows:

$$V_{des} = N_{cell}(\widehat{E_N} - V_{ohm} - V_{act} - V_{con}) \quad (31)$$

$$\widehat{E_N} = 1.229 - 0.85 * 10^{-3} \times (T - 298) + 4.3085 \times 10^{-5} \times T((lnPH_{2-FF}) + 0.5 \ln(PO_2)) \quad (32)$$

Substituting Eq. (32) in Eq. (31), then PH_{2-FF} will be given as in Eq. (33).

$$PH_{2-FF} = ln^{-1}\left(\frac{\left(\frac{V_{des}}{N_{cell}}\right)+V_{act}+V_{ohm}+V_{con}-1.229+\left(0.85*10^{-3}\right)(T-298)}{(4.3085*10^{-5})T} - 0.5 * \ln(PO_2)\right) \quad (33)$$

where V_{des}: is the desired input voltage. PH_{2-FF}: is the feedforward control action of the hydrogen partial pressure.

3.3 The Feedback Controller Design

The feedback controller is also necessary to stabilize the tracking voltage error of the Fuel Cell System when the output voltage of the PEMFC system is driftage from the required input voltage. Feedback controller consists of an on-line neural identifier and an optimization algorithm. The main goal of the feedback controller design is to find the feedback control action that minimizes the accumulative error between the desired voltage and output voltage of the PEMFC system as well as a weighted sum of the hydrogen partial pressure (PH_2) control signal. This can be achieved by minimizing the following multi-objective performance index as in Eq. (34) **Camacho and Bordons, 1999**.

$$J = \frac{1}{2}\sum_{k=1}^{N} Q(V_{des}(k+1) - V_{FC}(k+1))^2 + R(PH_{2-ref}(k) - PH_2(k))^2 \quad (34)$$

$PH_{2-ref}(k)$ is the reference control action of the hydrogen partial pressure and it is equivalent to $PH_{2-FF}(k)$. $PH_2(k)$: is the total control signal of the hydrogen partial pressure. $PH_{2-FB}(k)$: is the feedback control action of the hydrogen partial pressure.

$V_{des}(k+1)$: is the desired input voltage. (Q and R): are positive weighting coefficients. N: represents the number of steps ahead prediction. Hence:

$$PH_{2-ref}(k) = PH_{2-FF}(k) \quad (35)$$

$$PH_2(k) = PH_{2-FF}(k) + PH_{2-FB}(k) \quad (36)$$

Substituting Eq. (35) and Eq. (36) in Eq. (34) then J will be given as in Eq. (37).

$$J = \frac{1}{2}\sum_{k=1}^{N} Q(V_{des}(k+1) - V_{FC}(k+1))^2 + R(PH_{2-FF}(k) - (PH_{2-FF}(k) + PH_{2-FP}(k)))^2 \quad (37)$$

$$J = \frac{1}{2}\sum_{k=1}^{N} Q(V_{des}(k+1) - V_{FC}(k+1))^2 + R(PH_{2-FP}(k))^2 \quad (38)$$

This multi-objective cost function will not only force the output voltage to sequence the desired input voltage by minimizing the accumulative voltage error for N steps ahead but also compelling the control action of the hydrogen partial pressure in the transient period to be as close as potential to the reference control signal of the hydrogen partial pressure. Also, J depends on (R and Q) which are positive weighting coefficients, hence a control action of hydrogen partial pressure found will be optimal with respect to the given set of values of the weighting

factors *Q* and *R*. The choice of (*Q* & *R*) is done with engineering judgment and is often performed iteratively by observing the system response in the light of design specification such as overshoot and rise time **Ziogou et al., 2018, Camacho and Bordons, 1999**. The on-line identifier neural networks of the PEMFC system is to be used to obtain the predicted values of the output voltage of the system for N steps ahead instead of running the system itself N steps. These values are needed to calculate the feedback control action by the optimization algorithm such that the multi-objective performance index J will be minimized. Also, on-line identification is required to make $V_{FCm}(k)$ the output voltage of the identifier as close as possible to the PEMFC output $V_{FC}(k)$. A feedforward neural network is used as an identifier, and two stages of learning of this neural network will be performed: the off-line identification is considered as first stage, and an on-line modification of the weights of the obtained identifier to keep track of any possible variation of the PEMFC system parameters is considered as the second stage. Therefore it can be said $V_{FCm}(k) \approx V_{FC}(k)$, and performance index in Eq. (38) can be put as in Eq. (39):

$$J_m = \frac{1}{2}\sum_{k=1}^{N} Q(V_{des}(k+1) - V_{FCm}(k+1))^2 + R(PH_{2-FB}(k))^2 \quad (39)$$

$$J_m = \frac{1}{2}\sum_{k=1}^{N} Q(e_v(k+1))^2 + R(PH_{2-FB}(k))^2 \quad (40)$$

$$e_v(k+1) = V_{des}(k+1) - V_{FCm}(k+1) \quad (41)$$

In this work a one hidden layer feedforward neural network is used for the identifier, hence

$$V_{FCm}(k+1) = L(\sum_{a=1}^{Ah} W_a h_a + W_{Ah+1} \times bias) = L(neto) \quad (42)$$

where the activation function of the hidden layer is being a sigmoidal function but the output layer is a linear function.

CPSO algorithm is used to set the weights of the neural networks for learning the dynamics of the PEMFC, and a simple gradient descent rule is used. After the identifier learns the dynamics of the PEMFC system then the whole structure of the controller as shown in **Fig. 2** will be implemented.

3.3.1 One step ahead control action prediction

The feedback control signal of the hydrogen partial pressure $PH_{2-FB}(k+1)$ will be getting for one-step-ahead that is where N is equal to one.

$$PH_{2-FB}(k+1) = PH_{2-FB}(k) + \Delta PH_{2-FB}(k) \quad (43)$$

$$\Delta PH_{2-FB}(k) = -\eta \frac{\partial J_m}{\partial PH_{2-FB}(k)} \quad (44)$$

But:

$$-\eta \frac{\partial J_m}{\partial PH_{2-FB}(k)} = -\eta[\frac{\frac{1}{2}Q\partial(e_v(k+1))^2}{\partial PH_{2-FB}(k)} + \frac{\frac{1}{2}R\partial(PH_{2-FB}(k))^2}{\partial PH_{2-FB}(k)}] \quad (45)$$

By using the chain rule of differentiation, we will obtain the following:

$$\frac{\partial(e_v(k+1))^2}{\partial PH_{2-FB}(k)} = \frac{\partial(e_v(k+1))^2}{\partial V_{FCm}(k+1)} \times \frac{\partial V_{FCm}(k+1)}{\partial PH_{2-FB}(k)} = -2e_v(k+1) \times \frac{\partial V_{FCm}(k+1)}{\partial PH_{2-FB}(k)} \quad (46)$$

Hence, the equation (45) becomes as follows

$$-\eta \frac{\partial J_m}{\partial PH_{2-FB}(k)} = -\eta[-Qe_v(k+1)\frac{\partial V_{FCm}(k+1)}{\partial PH_{2-FB}(k)} + R(PH_{2-FB}(k))] \quad (47)$$

For the one hidden layer and one output layer of the on-line neural network identifier as be seen in **Fig. (4)** we will obtain the following:

$$\frac{\partial V_{FCm}(k+1)}{\partial PH_{2-FB}(k)} = \frac{\partial L(neto_b)}{\partial neto_b} \times \frac{\partial neto_b}{\partial PH_{2-FB}(k)} \tag{48}$$

For linear activation function in the output layer as $\frac{\partial L(neto_b)}{\partial neto_b} = 1$

$$\frac{\partial V_{FCm}(k+1)}{\partial PH_{2-FB}(k)} = 1 \times \frac{\partial neto_b}{\partial h_a} \times \frac{\partial h_a}{\partial PH_{2-FB}(k)} \tag{49}$$

$$\frac{\partial V_{FCm}(k+1)}{\partial PH_{2-FB}(k)} = 1 \times \sum_{a=1}^{Ah} W_a \frac{\partial h_a}{\partial net_a} \times \frac{\partial net_a}{\partial PH_{2-FB}(k)} \tag{50}$$

Where, $\frac{\partial h_a}{\partial net_a} = \frac{1}{2}\left[1-(h_a)^2\right] = H'(net_a)$ (51)

$$\frac{\partial V_{FCm}(k+1)}{\partial PH_{2-FB}(k)} = 1 \times \sum_{a=1}^{Ah} W_a \times H'(net_a) \times \frac{\partial net_a}{\partial PH_2(k)} \times \frac{\partial PH_2(k)}{\partial PH_{2-FB}(k)} \tag{52}$$

$$\frac{\partial V_{FCm}(k+1)}{\partial PH_{2-FB}(k)} = 1 \times \sum_{a=1}^{Ah} W_a \times H'(net_a) \times V_{an} \times \frac{\partial (PH_{2-FF}(k) + PH_{2-FB}(k))}{\partial PH_{2-FB}(k)} \tag{53}$$

$$\frac{\partial V_{FCm}(k+1)}{\partial PH_{2-FB}(k)} = 1 \times \sum_{a=1}^{Ah} W_a \times H'(net_a) \times V_{an} \times 1 \tag{54}$$

where the V_{an}'s are the weights of the $PH_2(k)$ only.

Hence,

$$\Delta PH_{2-FB}(k) = [\eta Q e_v(k+1) \sum_{a=1}^{Ah} (W_a \times H'(net_a) \times V_{an})] - [\eta \times R \times PH_{2-FB}(k)] \tag{55}$$

3.3.2 N steps ahead optimization algorithm

For N steps assessment of the neural feedback controller PH_{2-FB} the techniques of popularized predictive control theory will be used **Camacho and Bordons, 1999 and Al-Araji, et al., 2011**. The N-steps assessment of PH_{2-FB} is calculated for each specimen. Since, neural network identifier model as given by Eq. (17) represents the PEMFC model to be control approximately, were used to predict future values of the model output voltage for the future N steps, which used to detect the optimal value of PH_{2-FB} using an optimization algorithm. For this purpose, let N be a pre-specified positive integer and denote:

$$V_{dest,N} = [V_{des}(t+1), V_{des}(t+2), ..., V_{des}(t+N] \tag{56}$$

Where are future values of set point and t: represented the time instant, and

$$V_{FCmt,N} = [V_{FCm}(t+1), V_{FCm}(t+2), ..., V_{FCm}(t+N] \tag{57}$$

As the predicted outputs voltage of the identifier model of PEMFC system using the neural networks model in equation (17), then defined the following error voltage vector:

$$E_{vt,N} = [e_v(t+1), e_v(t+2), ..., e_v(t+N] \tag{58}$$

Where,

$$e_v(t+i) = V_{des}(t+i) - V_{FCm}(t+i) \text{ where, i=1, 2, … N} \tag{59}$$

Defining the feedback control signals PH_{2-FB} to be determined as follows:

$$PH'_{2-FBt,N} = [PH'_{2-FB}(t), PH'_{2-FB}(t+1),..., PH'_{2-FB}(t+N-1)] \quad (60)$$

Moreover, assuming the following multi-objective cost function:

$$J_N = \frac{1}{2} QE_{vt,N} E_{vt,N}{}^T + \frac{1}{2} RPH'_{2-FBt,N} PH'_{2-FBt,N}{}^T \quad (61)$$

Then our purpose is finding PH'_{2-FB} such as J_N represents the minimized by using the gradient descent rule, so that the new control action will be given by following:

$$PH'_{2-FBt,N}{}^{K+1} = PH'_{2-FBt,N}{}^{K} + \Delta PH'_{2-FBt,N}{}^{K} \quad (62)$$

Where *k* is indicating that calculations are achieved at the k^{th} sample; and

$$\Delta PH'_{2-FBt,N}{}^{K} = -\eta \frac{\partial J_N}{\partial PH'_{2-FBt,N}{}^{K}} = [\Delta PH'_{2-FB}(t), \Delta PH'_{2-FB}(t+1),...\Delta PH'_{2-FB}(t+N-1)] \quad (63)$$

$$-\eta \frac{\partial J_N}{\partial PH'_{2-FBt,N}{}^{K}} = \eta QE_{vt,N} \frac{\partial V_{FCmt,N}}{\partial PH'_{2-FBt,N}{}^{K}} - \eta RPH'_{2-FBt,N}{}^{K} \quad (64)$$

Where,

$$\frac{\partial V_{FCmt,N}}{\partial PH'_{2-FBt,N}{}^{K}} = \begin{bmatrix} \frac{\partial V_{FCm}(t+1)}{\partial PH'_{2-FB}(t)} & \frac{\partial V_{FCm}(t+2)}{\partial PH'_{2-FB}(t)} & \frac{\partial V_{FCm}(t+3)}{\partial PH'_{2-FB}(t)} & \cdots & \frac{\partial V_{FCm}(t+N)}{\partial PH'_{2-FB}(t)} \\ 0 & \frac{\partial V_{FCm}(t+2)}{\partial PH'_{2-FB}(t+1)} & \frac{\partial V_{FCm}(t+3)}{\partial PH'_{2-FB}(t+1)} & \cdots & \frac{\partial V_{FCm}(t+N)}{\partial PH'_{2-FB}(t+1)} \\ 0 & 0 & \frac{\partial V_{FCm}(t+3)}{\partial PH'_{2-FB}(t+2)} & \cdots & \frac{\partial V_{FCm}(t+N)}{\partial PH'_{2-FB}(t+2)} \\ : & : & : & : & : \\ 0 & 0 & 0 & 0 & \frac{\partial V_{FCm}(t+N)}{\partial PH'_{2-FB}(t+N-1)} \end{bmatrix} \quad (65)$$

It can be noted that each part in the above matrix could be found by differentiating the Eq. (17) with respect to each part in Eq. (60) as a result, it can be obtained that:

$$\frac{\partial V_{FCm}(t+n)}{\partial PH'_{2-FB}(t+j-1)} = \frac{\partial F_m(p)}{\partial PH'_{2-FB}(t+j-1)} + \sum_{i=m}^{n-1} \frac{\partial F_m(p)}{\partial V_{FCm}(t+i)} \times \left[\frac{\partial V_{FCm}(t+i)}{\partial PH'_{2-FB}(t+j-1)} \right]$$
$$n = 1,2,3,...,N$$
$$j = 1,2,3,...N \quad (66)$$

where *P* is the input pattern to the identifier neural networks.

$$P=[PH_2(t), PH_2(t-1),..., PH_2(t-n+1), V_{FC}(t), V_{FC}(t-1),..., V_{FC}(t-n+1)] \quad (67)$$

Eq. (65) represents the Jacobian matrix, which calculated by using Eq. (66) each time a new control signal PH_2 has to be determined. This could result in a large computation to large N. Therefore, a recursive method for calculating the Jacobian matrix is developing in the following, so the algorithm can be applied to real-time systems. After finishing the proceeding from n=1 to N and from j=1 to N the new control action PH_2 for the next sample will be

$$PH_2(k+1) = PH_{2-FF}(k+1) + PH'_{2-FB}{}^{K}(t+N) \quad (68)$$

where $PH'_{2-FB}{}^{k}(t+N)$ is last value of the feedback-controlling signal can be determined by using the optimization algorithm that N-step ahead of control signal is calculated.

This is calculated at every sample time *k* so $PH_2(k+1)$ is applied to that PEMFC system and the neural network identifier model at the next sampling time. Later, these steps were applied at the

next sampling time (k+1) until the voltage error between the required input voltage and the actual output voltage becomes less than a specified value. After each sampling time the weights of the on-line neural network identifier model are updated to minimize the model error between the actual PEMFC model and identifier model by using CPSO Algorithm.

4. NUMERICAL SIMULATION RESULTS

The suggested form of the predictive neural controller as explained in **Fig. 2** is carried out by using MATLAB m.file (2018) package. The first stage in the controller design is necessary to study and analyze the dynamic characteristics of the PEMFC system that it has the physical parameters, as shown in **Table 1**. The first study, is to show the polarization curve of the output voltage and the stack output power of the Fuel Cell in normal operation state during the load current is variable 0 A to 30 A while the hydrogen partial pressure is constant value at 1.0 bar, the oxygen partial pressure is constant value at 0.2 bar and the temperature of the operation is constant at 25C^{o} as in **Figs. (6, a and b)**.

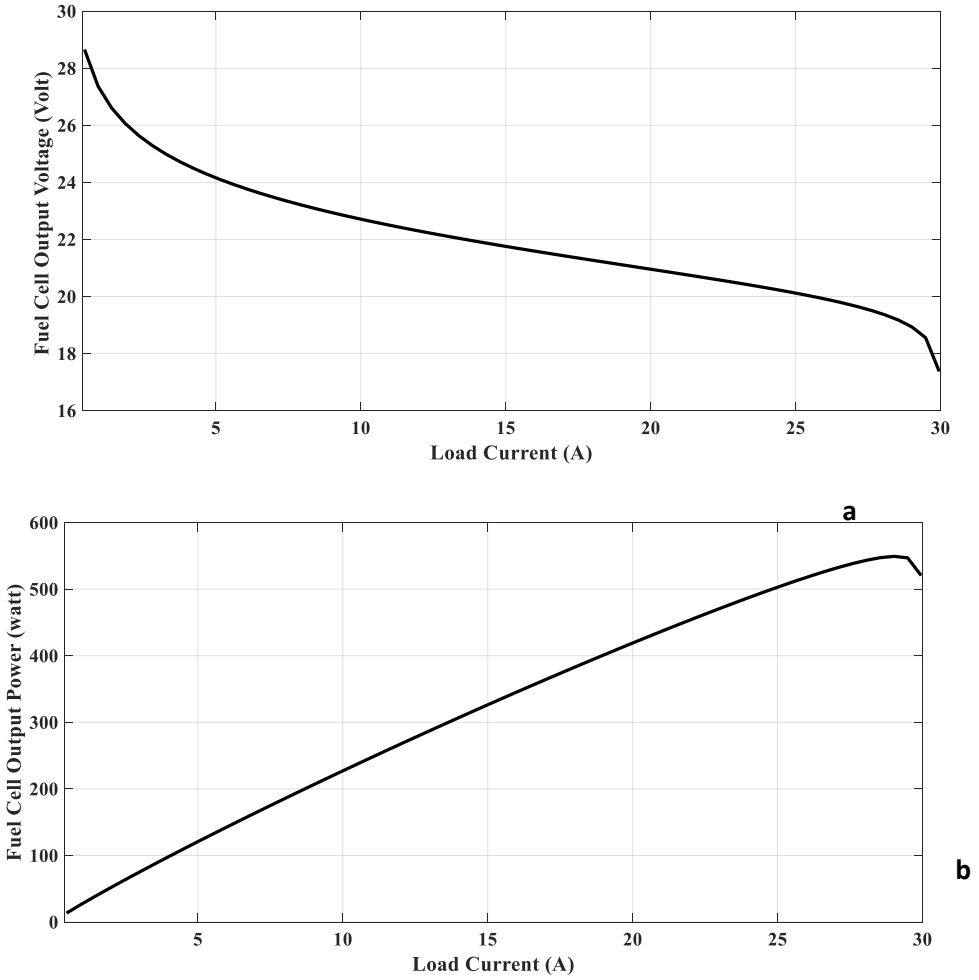

Figure 6 . a The output voltage of the fuel cell against load current variable, b) The fuel cell output power against load current variable.

The maximum power of this model is clear at the current which is equal to 29 A. **Fig. 7** shows the polarization curve of the loss voltage in the Fuel Cell system during the load current is variable from 0 A to 30 A. The second study is to show the effect of the hydrogen partial pressure changes from 0.1 bar to 5 bar on the output voltage of the Fuel Cell (FC) operation

during load current of (FC) is variable from 0 A to 30 A, while the temperature of the operation is constant at 25C°.

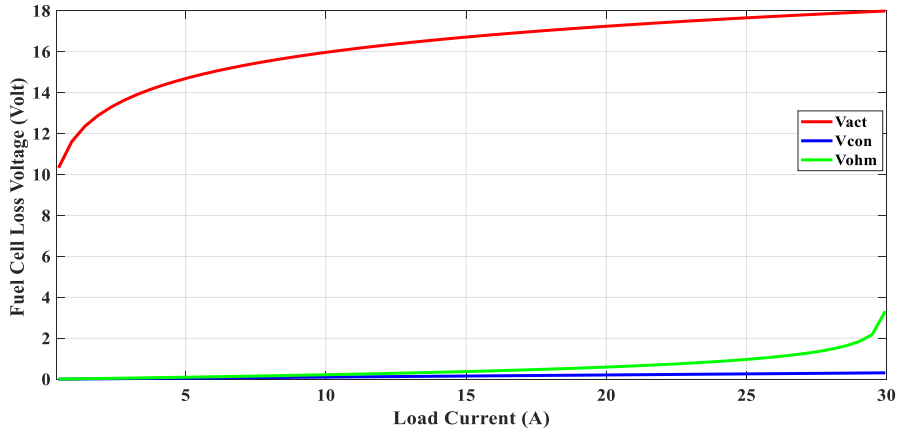

Figure 7. The drop voltage in the fuel cell system against load current variable.

Fig. 8 shows the output voltage of (FC) is increasing when the hydrogen partial pressure is increasing too. Because the thermodynamic potential (EN) value of the PEMFC system as in equation (6) has been improved toward increasing that led to the improved the performance of the Fuel Cell system. The third study is to show the effect of the temperature changes from 25 C° to 80 C° on the output voltage of (FC) operation during a load current of (FC) is variable from 0 A to 30 A while the hydrogen partial pressure is constant value at 1.0 bar and the oxygen partial pressure is constant value at 0.2 bar.

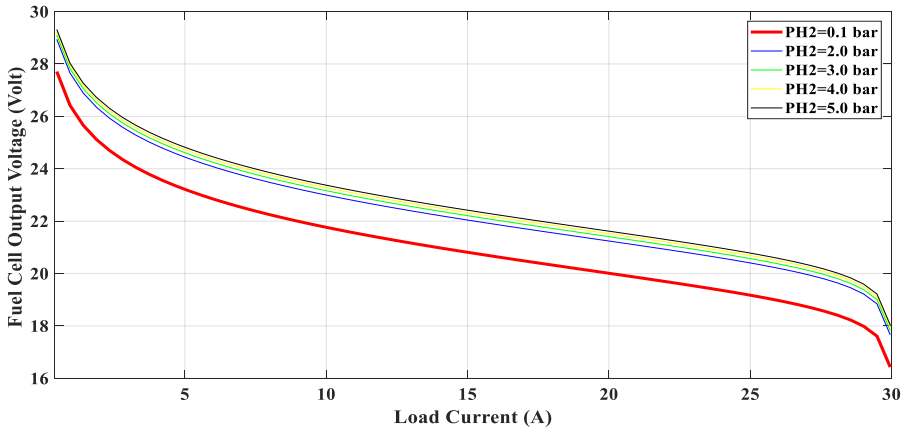

Figure 8. The fuel cell output voltage cell system against load current variable when the hydrogen partial pressure is changed against load current variable.

Fig. 9 shows the output voltage of (FC) is increasing when the temperature is increasing too. Because the thermodynamic potential (EN) value of the PEMFC system has been improved toward increasing and reducing the impact values of the parameters on the loss voltage in the fuel cell system, which led to improved performance of the fuel cell system. But when increasing the temperature of the operation of the fuel cell will cause loss of necessary humidity for the cell membranes that lead to a negative impact on the life of the fuel cell.

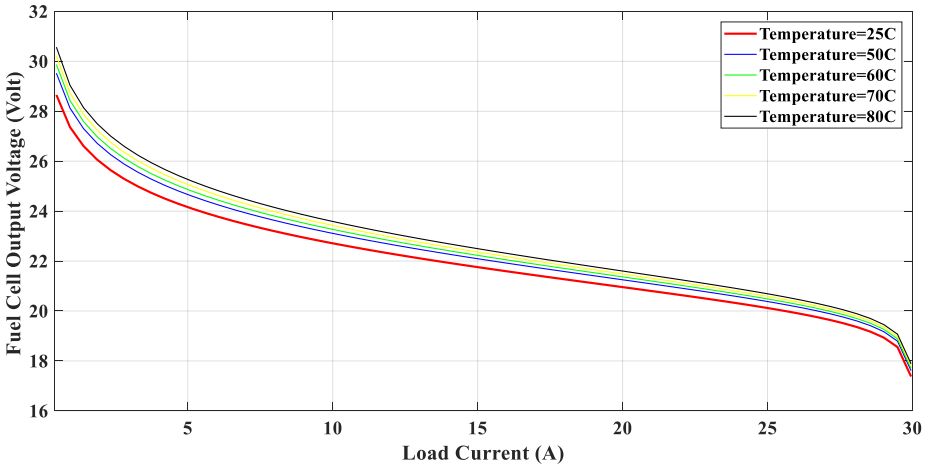

Figure 9. The fuel cell output voltage when the operation temperature is changed against load current variable.

To establish the proposed controller design, there are three stages should be achieved as follows: The first stage is to build the neural networks identifier PEMFC model, it is used the five steps for identification algorithm, as shown in **Fig. 3**. The first step is to generate input-output patterns, as shown in **Figs. 10, a and b** in order to excite all nonlinear regions of the fuel cell system and to show the dynamical behavior of it. Step two is using the MLP neural networks structure, as explained in **Fig. 4** to appear the PEMFC model system So the proposed number of the nodes in the three layers (input layer, hidden layer, and output layer) respectively are (5, 7, 1). Step three is using the CPSO algorithm to learn the neural network identifier model off-line algorithm; then it uses on-line algorithm to tune the identifier. Step four the proposed 2nd order dynamic behavior represents of the neural network identifier PEMFC model based on NARMA model as in Eq. (69).

$$V_{FCm}(k+1) = F_m[V_{FC}(k), V_{FC}(k-1), I(k), PH_2(k), PH_2(k-1)] \quad (69)$$

The signals entering to or sent out from the neural networks have been annealed to lie within (-1 and +1) to overcome numerical problems that are involved within real values. Scaling functions have to be added at the neural networks terminals (input-output) to transform the scaled values to actual values and vice versa. Because the inputs patterns (Load Current (1 to 25) A, and Hydrogen Partial Pressure (1 to 5) bar) and output patterns (Output Voltage (20 to 30) volt) are more significant than 1, as shown in **Figs. (10-a and b)**. After the learning cycle of the neural network identifier PEMFC model based on CPSO algorithm. The parameters of the off-line CPSO algorithm is identified as in **Table 2**.

Table 2. Parameters of off-line CPSO algorithm.

Number of Particles	Particle's weights	Max. inertia weight w_{max}	Min. inertia weight w_{min}	c_1 and c_2	r_1 and r_2	The best number of iteration
150	50	0.7	0.3	1.25	Random (0,1)	200

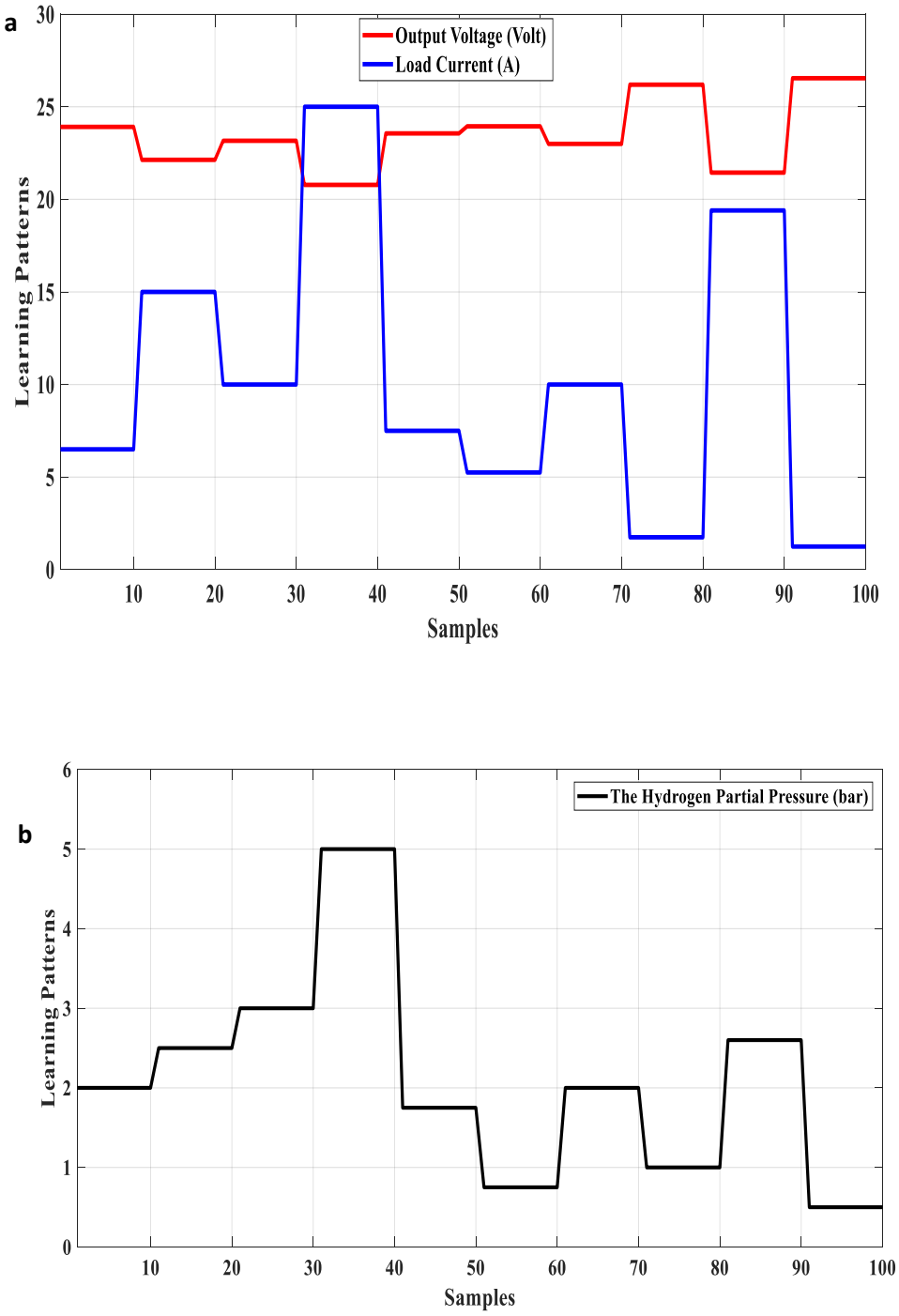

Figure 10. The learning set for the neural networks identifier PEMFC model a) voltage and load current set, b) the hydrogen partial pressure set.

Fig. 11 shows the excellent responses of neural networks identifier PEMFC model with the actual output voltage of (FC) system in learning mode and model error is zero approximation for 100 patterns.

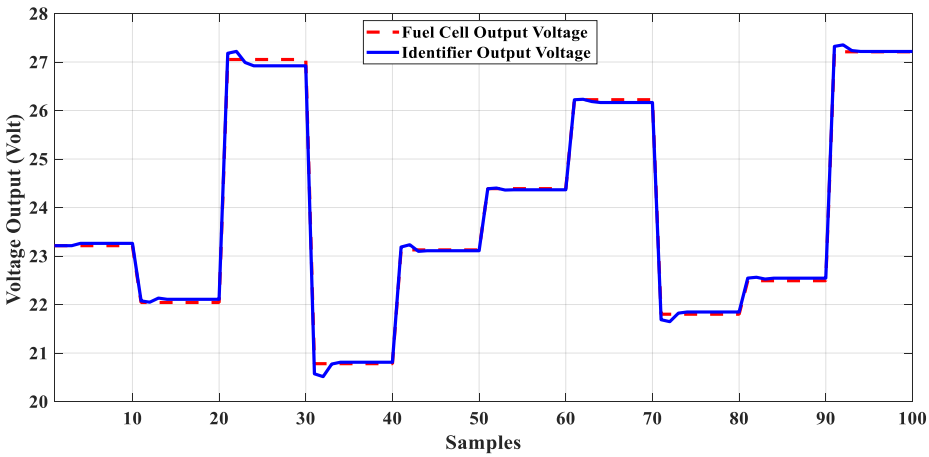

Figure 11. The output voltage of the fuel cell system and neural networks identifier model for learning set.

Based on CPSO algorithm, the off-line mean square error is shown in **Fig. 12** that it has the minimum value of the performance index and reaching to 0.0036.

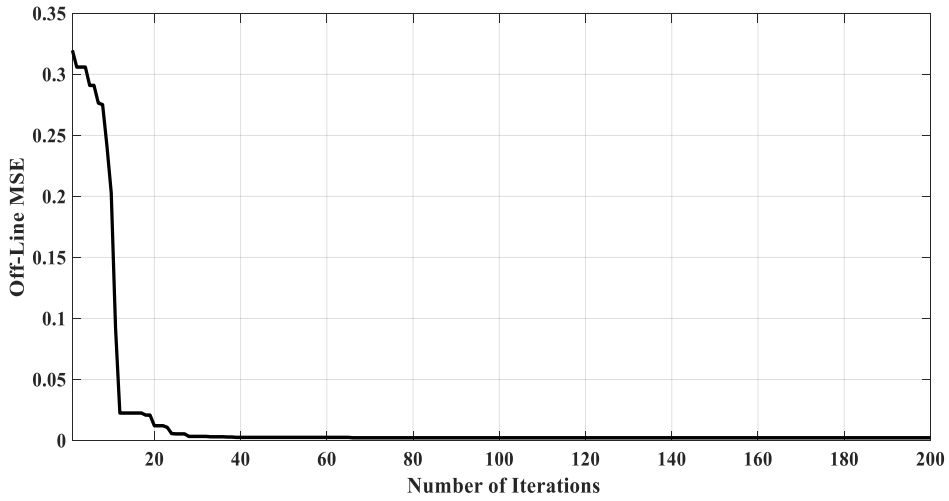

Figure 12. The off-line mean square error cost function for learning identifier PEMFC model.

The five-step is model validation and it can be achieved by using 100 new patterns as a testing pattern for the neural networks identifier PEMFC model. The responses of neural networks identifier PEMFC model followed the actual output voltage of (FC) and without the over learning problem occurred in the learning cycle for CPSO algorithm as shown in **Fig. 13**.

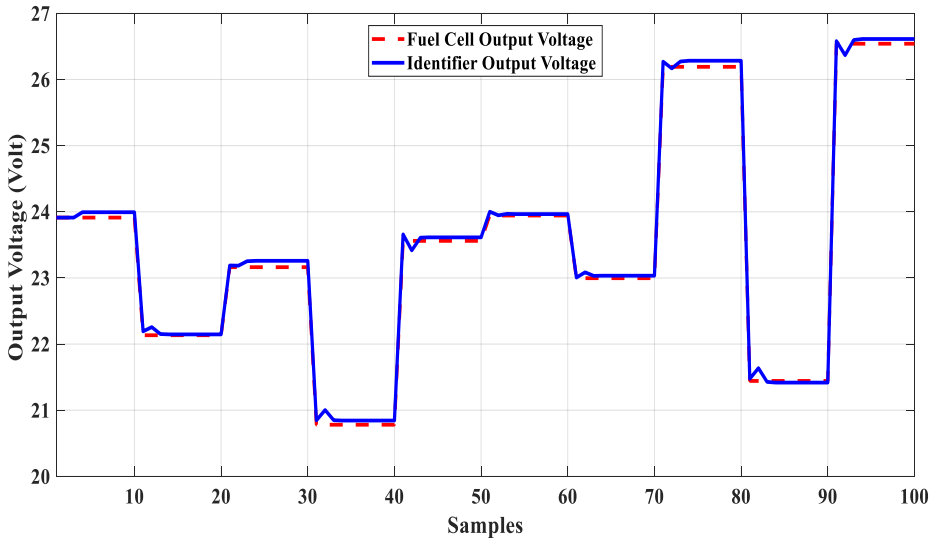

Figure 13. The output voltage of the fuel cell system and neural networks identifier model for testing set.

The second stage calculates the reference hydrogen partial pressure control action based on the proposed numerical feedforward controller design as in Eq. (33) in order to keep the tracking voltage error of the fuel cell system to zero value at steady-state. The third stage is a neural feedback controller design; it can be implemented based on neural network identifier PEMFC model and multi-objective cost function. So the feedback hydrogen partial pressure control action for one-step-ahead is represented as in Eq. (43). To confirm the proposed controller design can generate the optimal hydrogen partial pressure control operation and to track the desired output voltage of PEMFC system as precisely and quickly. On-line CPSO algorithm is using to tune the weights of the neural networks identifier PEMFC model and parameters of on-line CPSO algorithm can be defined as in **Table 3**.

Table 3. Parameters of on-line CPSO algorithm.

Number of Particles	Particle's weights	Max. inertia weight w_{max}	Min. inertia weight w_{min}	c_1 and c_2	r_1 and r_2	The best number of iteration
20	50	0.7	0.3	1.25	Random (0,1)	20

The 125 samples that represent the five different step-change desired outputs voltages of the PEMFC system with five cases of variable load current are carried out as shown in **Fig. 14**.

Fig 15. shows that, for one-step-ahead prediction, the actual output voltage of the PEMFC system is suitable tracking the desired output voltage for the five different step-change without oscillation in the output, the steady-state error is not equal to zero value, and it has overshoot in the start sample because of the initial output voltage of the PEMFC system.
While for ten step-ahead predictions, the actual output voltage of the PEMFC system is excellent tracking the desired output voltage for the five different step-change without oscillation in the output. The steady-state error is equal to zero value, and no overshoot in the start sample because of the controller design with optimization algorithm could process the difference voltage between the initial output voltage of the PEMFC system and the desired output voltage.

Fig. 16. shows that, the response of the hydrogen partial pressure control action for one-step-ahead prediction of the proposed neural predictive controller. It has not smooth control action of the partial pressure to track the desired output voltage, and it tries to minimize the steady-state error to the zero value. While for ten step-ahead predictions, the optimal response of the hydrogen partial pressure control action has smooth control action to track the desired output voltage and it approximates to minimize the steady-state error to the zero value when we are taken the (Q and R) parameters are equal to (10 and 1) respectively.

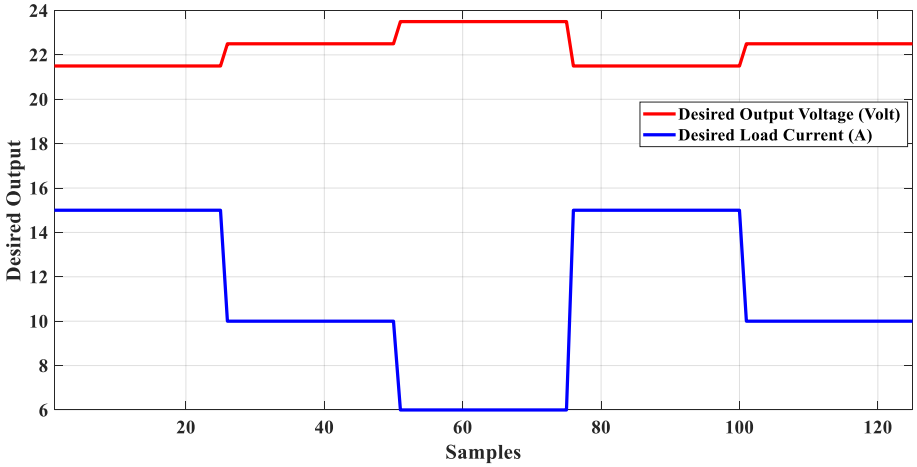

Figure 14. The desired output voltage and load current for the fuel cell system.

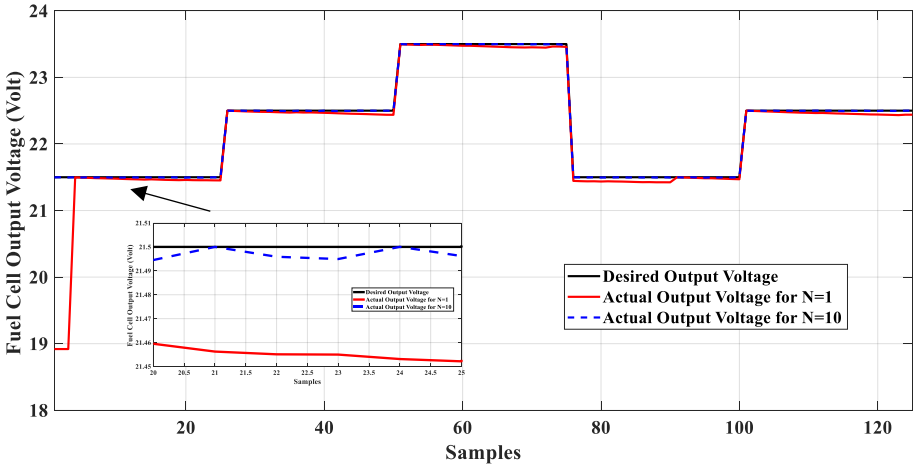

Figure 15. The actual output voltage of the fuel cell for one-step ahead and ten-step ahead prediction.

To analyze the effectiveness of the two parameters (Q and R) in the controller design, **Fig. 17** shows the 3-D response of the values of the on-line multi-objective cost function with respect to (Q and R) parameters for one-step-ahead prediction. It is clear that when increasing the value of the Q parameter (from 1 to 10) and decreasing the value of the R parameter (10 to 1), the on-line multi-objective cost function value is decreasing that depends on the Eq. (55) which is generated the step change value of the feedback control effort.

The proposed controller behavior is more accurate for tracking the output voltage of the fuel cell in the transient state and in the steady-state and made the error value equal to zero approximation with a minimum value of the on-line multi-objective cost function and reducing the number of the fitness evaluation at ten-step ahead prediction, as shown in **Fig. 18**.

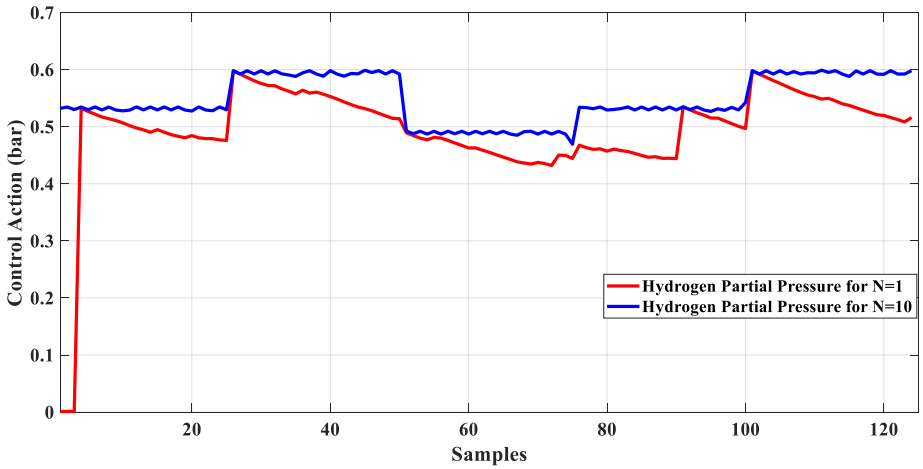

Figure 16. The control effort for one-step ahead and ten-step ahead prediction.

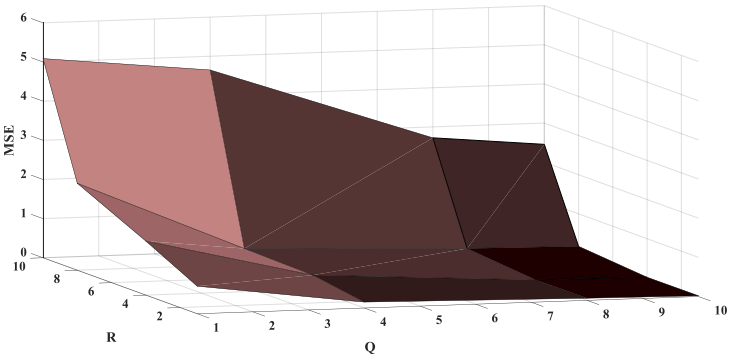

Figure 17. The 3-D response of the values of the on-line multi-objective cost function.

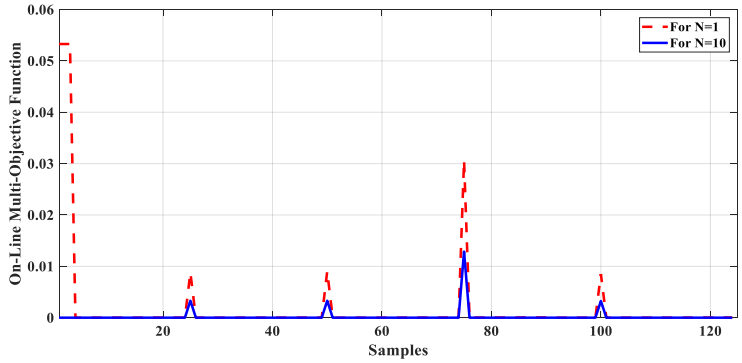

Figure 18. The on-line performance of the multi-objectives for one-step ahead and ten-step ahead prediction.

CONCLUSIONS

The numerical simulation results of the suggested neural predictive controller with CPSO algorithm for modeling and controlling the nonlinear PEMFC system are presented in this paper. The proposed neural predictive N-step ahead algorithm has many abilities in terms of (i) Strong adaption algorithm to build neural network identifier PEMFC model without over-learning problem; (ii) Fast and smooth learning and tuning algorithm which leads to no oscillation in the output neural network identifier model; (iv) High robustness behavior for neural predictive controller when generated the hydrogen partial action to follow the desired output voltage of the PEMFC system during the load current is variation especially when used ten step-ahead prediction.

REFERENCES

- Abbaspour, A., Khalilnejad, A., and Chen, Z., 2016, "Robust Adaptive Neural Network Control for PEM Fuel Cell". International Journal of Hydrogen Energy, Vol. 41, No. 44, pp. 20385-20395.
- Al-Araji, A. S., 2014, "A Comparative Study of Various Intelligent Algorithms Based Nonlinear PID Neural Trajectory Tracking Controller for the Differential Wheeled Mobile Robot Model". Journal of Engineering, Vol. 20, No. 5, pp. 44-60.
- Al-Araji, A. S., 2015, "A Cognitive PID Neural Controller Design for Mobile Robot Based on Slice Genetic Algorithm". Engineering & Technology Journal, Vol. 33, No.1, pp. 208-222.
- Al-Araji, A. S., 2016, "Cognitive non-linear controller design for magnetic levitation system". Transactions of the Institute of Measurement and Control, Vol. 38, No. 2, pp. 215-222.
- Al-Araji, A. S., Abbod, M. F., and Al-Raweshidy, H. S., 2011, "Design of a neural predictive controller for nonholonomic mobile robot based on posture identifier". Proceedings of the IASTED International Conference Intelligent Systems and Control (ISC 2011), Cambridge, United Kingdom, pp. 198-207.
- Al-Araji, A. S., Abbod, M. F., and Al-Raweshidy, H. S., 2011,"Design of an adaptive nonlinear PID controller for nonholonomic mobile robot based on posture identifier". IEEE International Conference on Control System, Computing and Engineering (ICCSCE), pp. 337-342.
- Al-Araji, A. S., Abbod, M. F., and Al-Raweshidy, H. S., 2011,"Neural autopilot predictive controller for nonholonomic wheeled mobile robot based on a pre-assigned posture identifier in the presence of disturbances". The 2nd International Conference on Control, Instrumentation and Automation (ICCIA), pp. 326-331.
- Ali, E., Abudhahir, A., and Boopathi, M., 2018,"Firefly Algorithm Tuned PI Controller for Pressure Regulation in PEM Fuel Cells". Journal of Computational and Theoretical Nanoscience, Vol. 15, No. 3, pp. 845-853.
- Askarzadeh, A., and Rezazadeh, A., 2011,"A New Artificial Bee Swarm Algorithm for Optimization of Proton Exchange Membrane Fuel Cell Model Parameters". Journal of Zhejiang University-Science C (Computers & Electronics), Vol. 12, No. 8, pp. 638-646.

- Beirami, H., Shabestari, A. and Zerafat, M., 2015, "Optimal PID Plus Fuzzy Controller Design for A PEM Fuel Cell Air Feed System Using the Self-Adaptive Differential Evolution Algorithm". International Journal of Hydrogen Energy, Vol. 40, No. 30, pp. 9422-9434.
- Benchouia, N., Derghal, A., Mahmah, B., Madi, B., Khochemane, L., and Aoul, E., 2015. "An Adaptive Fuzzy Logic Controller (AFLC) for PEMFC Fuel Cell". International Journal of Hydrogen Energy, Vol. 40, No. 39, pp. 13806-13819.
- Camacho, E. F., and Bordons, C., 1999, "Model Predictive Control". London: Springer-Verlag.
- Corrêa, J., Farret, F., Gomes, J., and Simões, M., 2003."Simulation of Fuel-Cell Stacks Using a Computer-Controlled Power Rectifier With the Purposes of Actual High-Power Injection Applications". IEEE Transactions on Industry Applications, Vol. 39, No. 4, pp. 1136-1142.
- Dagher, K. E., 2018, "Design of an Adaptive Neural Voltage-Tracking Controller for Nonlinear Proton Exchange Membrane Fuel Cell System based on Optimization Algorithms". Journal of Engineering and Applied Sciences. Vol. 13, No. 15, pp. 6188-6198.
- Damour, C., Benne, M., Perez, B., and Chabriat, J., 2014, "Neural Model-Based Self-Tuning PID Strategy Applied to PEMFC". Engineering, Vol. 6, pp. 159-168.
- Daud, W., Rosli, R., Majlan, E., Hamid, S., and Mohamed, R., 2017, "PEM Fuel Cell System Control: A Review". Renewable Energy, Vol. 113, No. 19, pp. 620-638.
- Derbeli, M., Farhat, M., Barambones, O., and Sbita, L., 2017,"Control of PEM Fuel Cell Power System Using Sliding Mode and Super-Twisting Algorithms". International Journal of Hydrogen Energy, Vol. 42, No. 13, pp. 8833-8844.
- El-Sharkh, M., Rahman, A., and Alam, M., 2004, "Neural Networks-based Control of Active and Reactive Power of a Stand-Alone PEM Fuel Cell Power Plant". Journal of Power Sources, Vol. 135, pp. 88-94.
- Isa, Z., and Rahim, N., 2013, "PEM Fuel Cell Model Parameters Optimization Using Modified Particle Swarm Optimization Algorithm". IEEE Conference on Clean Energy and Technology (CEAT), pp. 442-445.
- Kumar, P., Kannaiah, S., Choudhury, S., and Rajasekar, N., 2017, "Genetic Algorithm-Based Modeling of PEM Fuel Cells Suitable for Integration in DC Microgrids". Electric Power Components and Systems, Vol. 45, No. 10, pp. 1152-1160.
- Li, P., Chen, J., Cai, T., and Zhang, B., 2011, "Adaptive Control of Air Delivery System for PEM Fuel Cell Using Backstepping". The 8th Asian Control Conference (ASCC), pp. 1282-1287.
- Liua, J., Linc, W., Alsaadid, F., and Hayatd, T., 2015, "Nonlinear Observer Design for PEM Fuel Cell Power Systems via Second Order Sliding Mode Technique". Neurocomputing, Vol. 168, No. C, pp. 145-151.
- Manikandana, T., and Ramalingamb, S., 2016, "A review of Optimization Algorithms for the Modeling of Proton Exchange Membrane Fuel Cell". Journal of Renewable Sustainable Energy, Vol. 8, pp. 034301-034314.
- Nells, O., 2001, "Nonlinear System Identification". Springer – Verlag Berlin Heidelberg.

- Rajasekar, N., Jacob, B., Balasubramanian, K., Sangeetha, K., and Babu, T., 2015, "Comparative Study of PEM Fuel Cell Parameter Extraction using Genetic Algorithm". Ain Shams Engineering Journal, Vol. 6, pp. 1187-1194.
- Salim, R., Noura, H., and Fardoun, A., 2013, "A Parameter Identification Approach OF A PEM Fuel Cell Stack Using Particle Swarm Optimization". ASME, 11th Fuel Cell Science, Engineering and Technology Conference, pp. 1-8.
- Ziogou, C., Voutetakis, S., Georgiadis, M., and Papadopoulou, S., 2018, "Model Predictive Control (MPC) Strategies for PEM Fuel Cell Systems - A Comparative Experimental Demonstration". Chemical Engineering Research and Desgin, Vol. 131, pp. 656-670.
- Ziogoua, C., Papadopouloua, S., Georgiadis,M., and Voutetakis, S., 2013, "On-Line Nonlinear Model Predictive Control of A PEM Fuel Cell System". Journal of Process Control, Vol. 23, pp. 483-492.